crystallographic data are collected in Table VII.

$W(OC_6H_3PhC_6H_4)_2(PMePh_2)_2$ (2b). An approximately equi-dimensional crystal was mounted by using silicone grease and was transferred to a goniostat where it was cooled to −140 °C for characterization and data collection. Space group $P2_2/c$ was assigned based on systematic absences. Four standards measured every 300 data showed no significant trends. The residual for the averaging of redundant data was 0.11 for 799 intensities observed more than once. The data contained a large number of weak intensities, almost half of the 6587 unique data being less than 2.33σ.

The structure was solved by a combination of direct methods (MULTAN78) and Fourier techniques. Following the location of the atoms in the molecule of interest, a difference map revealed four unique peaks near a crystallographic center of symmetry which formed an apparent molecule of *p*-xylene. These atoms did not refine well, but insofar as they could be refined, the occupancy of the terminal atom appears less than the atoms in the ring. Therefore the unit cell most likely contains $^1/_2$ molecule of disordered toluene. No attempt was made to locate hydrogens on this molecule.

Attempts to refine all non-hydrogen atoms anisotropically were unsuccessful, probably due to the large amount of weak data. Tungsten, phosphorous, and oxygen atoms were refined anisotropically, and carbon atoms were refined isotropically. Hydrogens were placed in calculated positions prior to the final cycles of least-squares refinement which gave a final $R = 0.0615$ for 3313 unique data $\geq 2.33\ \sigma$. The final difference map had no additional peaks of significance. There were three residual peaks of 1.0–1.5 e/A^3 in the vicinity of the tungsten atom, and all others were less than 1 e/A^3.

$W(OC_6H_3Ph\text{-}\eta^6\text{-}C_6H_5)(OAr\text{-}2,6\text{-}Ph_2)(PMePh_2)$ (3). The particular sample consisted of two components, yellow crystals, which were the bulk of the sample (in the particular tube examined), and green crystals. The present study was undertaken on one of the green crystals. A suitable well-formed green crystal was located and transferred to the goniostat by using standard inert-atmosphere handling techniques employed by the IUMSC and cooled to −155 °C for characterization and data collection.

A systematic search of a limited hemisphere of reciprocal space located a set of diffraction maxima with no symmetry or systematic absences corresponding to one of the triclinic space groups. Subsequent solution and refinement of the structure confirmed the centrosymmetric choice, $P\bar{1}$.

Data were collected in the usual manner by using a continuous θ–2θ scan with fixed backgrounds. Data were reduced to a unique set of intensities and associated σ's in the usual manner. The structure was solved by a combination of Patterson techniques and Fourier techniques. The positions of most of the hydrogen atoms were clearly visible in a difference Fourier phased on the non-hydrogen atoms and were included as fixed atom contributors in the final cycles of refinement.

A final difference Fourier was essentially featureless, with the largest peak being 0.85 e/A^3.

$W(OC_6H_3Ph\text{-}\eta^6\text{-}C_6H_5)(OAr\text{-}2,6\text{-}Ph_2)(dppm)$ (4). A suitable crystal of compound 4 was examined under deoxygenated Nujol and mounted in a appropriate sized glass capillary surrounded by epoxy resin. The hydrogen atom positions were calculated after several cycles of anisotropic refinement assuming idealized geometries and a carbon–hydrogen bond distance of 0.95 Å. For the methyl groups, one hydrogen position was located in a difference Fourier map, this position idealized, and the other two hydrogen positions calculated. Hydrogens were drawn with an arbitrary radius and were not refined. No correction for extinction was applied.

Acknowledgment. We thank the National Science Foundation (Grant CHE-8612063 to I.P.R.) for financial support of this work as well as for support of the Crystallographic Center at Purdue.

Supplementary Material Available: Tables of anisotropic thermal parameters and full bond distances and angles for **2b**, **3**, and **4** (32 pages); listings of observed and calculated structure factor tables for **2b**, **3**, and **4** (57 pages). Ordering information is given on any current masthead page.

Thermodynamics for the Addition of $[(OEP)Rh]_2$ with Propene and Observation of a Facile Dyotropic 1,2 Exchange of (OEP)Rh Groups in $(OEP)Rh{-}CH_2CH(CH_3){-}Rh(OEP)$

Bradford B. Wayland,* Yuping Feng, and Sujuan Ba

Department of Chemistry, University of Pennsylvania, Philadelphia, Pennsylvania 19104-6323

Received August 29, 1988

(Octaethylporphyrin)rhodium(II) dimer, $[(OEP)Rh]_2$ (1), reacts with propene to form $(OEP)Rh{-}CH_2CH(CH_3){-}Rh(OEP)$ (2). Thermodynamic values for the addition reaction were measured in benzene by NMR methods ($\Delta H° = -9.5 \pm 1.0$ kcal mol^{-1}; $\Delta S° = -20 \pm 5$ cal K^{-1} mol^{-1}) and used in estimating an average Rh–C bond dissociation energy of ~45 kcal mol^{-1} in 2. Facile stereospecific 1,2 interchange of (OEP)Rh groups was observed for 2, and the activation parameters for this dyotropic process were determined by NMR line-shape analysis ($\Delta H^* = 12.4 \pm 0.5$ kcal mol^{-1}; $\Delta S^* = -10.7 \pm 1.9$ cal K^{-1} mol^{-1}).

Introduction

Addition reactions of (octaethylporphyrin)rhodium(II) dimer, $[(OEP)Rh]_2$ (1), with alkenes produce alkyl-bridged complexes (eq 1).[1,2] Both thermodynamic and kinetic studies for reaction 1 using styrene in benzene have been reported by Halpern.[2] Results from kinetic studies were used to implicate the metallo radical $[(OEP)Rh]^\bullet$ in a radical chain mechanism described by eq 2–4.[2] This paper reports on the thermodynamic values for reaction 1 using

$$[(OEP)Rh]_2 + CH_2{=}CH(X) \rightleftarrows (OEP)Rh{-}CH_2CH(X){-}Rh(OEP) \quad (1)$$

$$[(OEP)Rh]_2 \rightleftarrows 2[(OEP)Rh]^\bullet \quad (2)$$

$$(OEP)Rh^\bullet + CH_2{=}CH(C_6H_5) \rightleftarrows (OEP)Rh{-}CH_2\dot{C}H(C_6H_5) \quad (3)$$

$$(OEP)Rh{-}CH_2\dot{C}H(C_6H_5) + [(OEP)Rh]_2 \rightarrow (OEP)Rh{-}CH_2CH(C_6H_5){-}Rh(OEP) + [(OEP)Rh]^\bullet \quad (4)$$

---

[1] (a) Ogoshi, H.; Setsume, J.; Yoshida, Z. *J. Am. Chem. Soc.* **1977**, *99*, 3869. (b) Del Rossi, K. J.; Wayland, B. B *J. Chem. Soc., Chem. Commun.* **1986**, 1653.

[2] Paonessa, R. S.; Thomas, N. C.; Halpern, J. *J. Am. Chem. Soc.* **1985**, *107*, 4333.

0276-7333/89/2308-1438$01.50/0

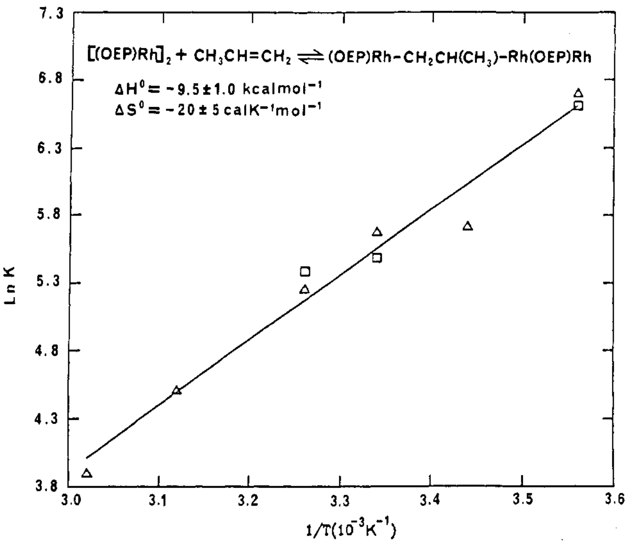

Figure 1. Van't Hoff plot for the addition reaction of [(OEP)Rh]$_2$ with CH$_2$=CH—CH$_3$ to form (OEP)Rh-CH$_2$CH(CH$_3$)-Rh(OEP) in C$_6$D$_6$ solution: △, [[(OEP)Rh]$_2$]$_i$ = 2.88 × 10^{-3} M and [CH$_2$=CHCH$_3$] (298 K) = 9.40 × 10^{-3} M; □, [[(OEP)Rh]$_2$]$_i$ = 2.62 × 10^{-3} M and [CH$_2$=CHCH$_3$] (298 K) = 6.55 × 10^{-3} M.

propene and on a kinetic–mechanistic study of a 1,2 interchange of (OEP)Rh units in (OEP)Rh-CH$_2$CH(CH$_3$)-Rh(OEP) (2).

Results

Benzene solutions of [(OEP)Rh]$_2$ (1) react with propene ($P_{C_3H_6}$ = 0.1–0.5 atm) to produce an equilibrium distribution with (OEP)Rh-CH$_2$CH(CH$_3$)-Rh(OEP) (2) (eq 5).

$$[(OEP)Rh]_2 + CH_2{=}CH(CH_3) \rightleftarrows (OEP)Rh{-}CH_2CH(CH_3){-}Rh(OEP) \quad (5)$$

Two distinct sets of porphyrin ^{1}H NMR resonances corresponding to the nonequivalent (OEP)Rh units in 2 are observed at temperatures below 295 K. The high-field positions for the alkyl hydrogen resonances (CH$_{(1)}$ (–11.25 ppm), CH$_{(2)}$ (–10.36 ppm), CH$_{(3)}$ (–9.89 ppm), CH$_{3(4)}$ (–8.68 ppm)) are caused by the combined ring current effects from two (OEP)Rh units and the pattern of coupling constants ($J_{1,2}$ (6.8 Hz), $J_{1,3}$ (<2 Hz), $J_{2,3}$ (11.6 Hz), $J_{3,4}$ (6.0 Hz)) results from the expected trans arrangement of (OEP)Rh groups in the preferred conformation of 2.

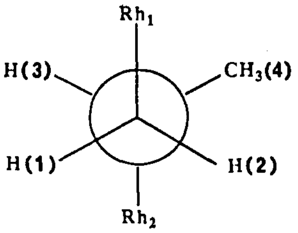

Temperature dependence of the integrated intensity of the methine hydrogens in 1, 2, and each of the alkene hydrogens of propene have been used in evaluating thermodynamic parameters for reaction 5 ($\Delta H°_5$ = –9.5 ± 1.0 kcal mol^{-1}; $\Delta S°_5$ = –20 ± 5 cal K^{-1} mol^{-1}) (Figure 1).

When benzene solutions containing 1, 2, and propene are heated at temperatures above 350 K for several hours, additional reactions occur that produce equal quantities of (OEP)Rh—CH$_2$CH=CH$_2$ (3) and (OEP)Rh—CH$_2$CH$_2$CH$_3$ (4). Assignments for compounds 3 and 4 are based on independent syntheses from the reactions of (OEP)Rh$^-$ with ClCH$_2$CH=CH$_2$ and BrCH$_2$CH$_2$CH$_3$, respectively. Compound 4 has also been obtained by the addition of (OEP)Rh–H with propene. The reactions that occur subsequent to formation of 2 are slow compared to the time required to equilibrate 1 with 2 and thus do not interfere with the thermodynamic study of reaction 5.

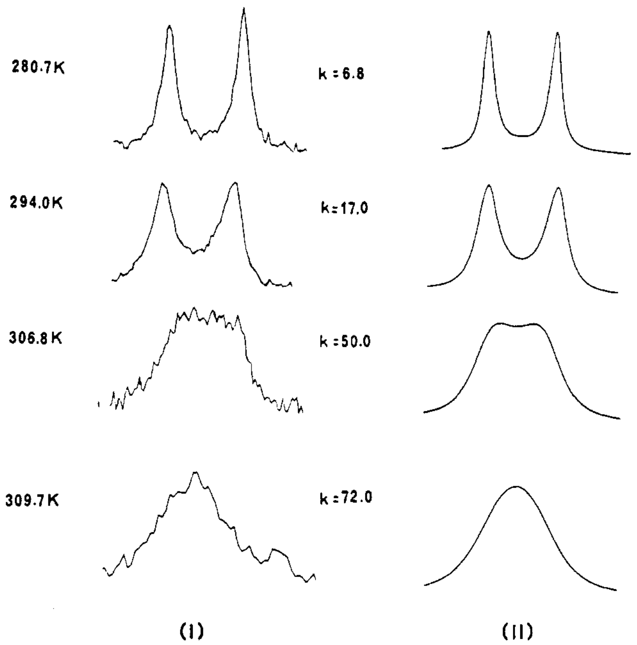

Figure 2. Temperature dependence for the methine porphyrin hydrogens in (OEP)Rh-CH$_2$CH(CH$_3$)-Rh(OEP): (I) observed; (II) simulated for two-site exchange using ΔH^* = 12.4 kcal mol^{-1} and ΔS^* = –10.7 cal K^{-1} mol^{-1}.

Temperature dependence of the ^{1}H NMR for the porphyrin methine hydrogens of 2 are illustrated in Figure 2. Broadening and subsequent merging of these porphyrin resonances as the temperature increases (270–320 K) indicate that the nonequivalent (OEP)Rh groups are exchanging. Full line-shape analysis for the methine ^{1}H NMR spectra at a series of temperatures results in the activation parameters (ΔH^* = 12.4 ± 0.5 kcal mol^{-1}; ΔS^* = –10.7 ± 1.9 cal K^{-1} mol^{-1}) for the exchange process. Throughout this same temperature range no changes are observed for the coupling patterns of the high-field alkyl ^{1}H NMR peaks, which indicates that the 1,2 interchange of (OEP)Rh groups does not change the structural relationship of H$_{(3)}$ with H$_{(1)}$ and H$_{(2)}$ (Figure 3).

Discussion

Reactions of [(OEP)Rh]$_2$ with Propene. [(OEP)Rh]$_2$ (1) reacts with excess propene in C$_6$D$_6$ to produce (OEP)Rh-CH$_2$CH(CH$_3$)-Rh(OEP) (2) as the exclusive initial product observed (eq 5). Reaction 5 presumably occurs by a metallo radical chain mechanism like that implicated in the corresponding reaction of styrene[2] (eq 2-4). Reaction of the intermediate radical (OEP)Rh-CH$_2\dot{C}$H(CH$_3$) with [(OEP)Rh]$_2$ is apparently faster than either disproportionation or propene oligomerization reactions. Further slow reactions do occur over a period of days at 295 K or several hours at 350 K that convert 2, in the presence of excess propene, into equal amounts of (OEP)Rh—CH$_2$CH=CH$_2$ (3) and (OEP)Rh—CH$_2$CH$_2$CH$_3$ (4) (eq 6). Formation of compounds 3 and 4 could result

$$(OEP)Rh{-}CH_2CH(CH_3){-}Rh(OEP) + CH_3CH{=}CH_2 \rightarrow (OEP)Rh{-}CH_2{-}CH{=}CH_2 + (OEP)Rh{-}CH_2CH_2CH_3 \quad (6)$$

from disproportionation of the organometallic radical (OEP)Rh—CH$_2\dot{C}$H(CH$_3$) that is continually produced by the reverse of reaction 5.

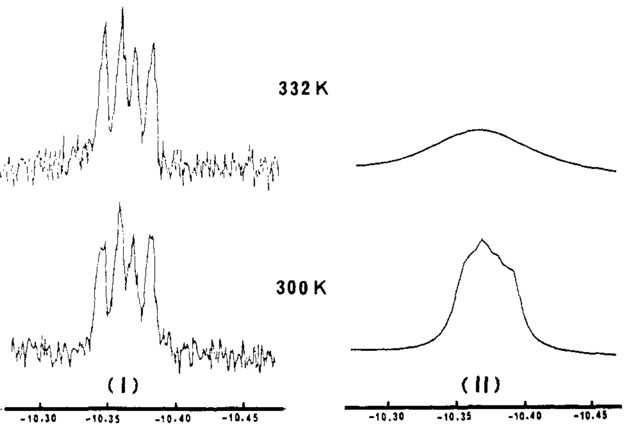

Figure 3. 500-MHz ^{1}H NMR spectra for the $H_{(2)}$ resonance in compound 2: (I) observed $H_{(2)}$ spectrum; (II) simulated $H_{(2)}$ spectrum assuming site exchange between the diastereotopic hydrogens ($H_{(1)}$ and $H_{(2)}$) at a rate that is one-half of the rate for 1,2 (OEP)Rh exchange in compound 2.

Thermodynamic Study. Equilibration of 2 with 1 and propene is fast relative to subsequent reactions which permits measurement of the thermodynamic parameters for reaction 5 in C_6D_6 ($\Delta H°_5 = -9.5 \pm 1.0$ kcal mol^{-1}; $\Delta S°_5 = -20 \pm 5$ cal K^{-1} mol^{-1}). Thermodynamic values for the addition of 1 to propene (eq 5) are similar to those reported by Halpern for the corresponding reaction of 1 with styrene ($\Delta H° = -11.2 \pm 2.5$ kcal mol^{-1}, $\Delta S° = -15 \pm 8$ cal K^{-1} mol^{-1}).[2]

The general addition reaction of a M–M bonded complex with $CH_2{=}CH(R)$ (eq 7) has been analyzed in terms of approximate bond energies for the reactants and products (eq 8–10).[3] Evaluation of the approximate enthalpy relationship (eq 9) for the specific case of (OEP)Rh species where the Rh–Rh bond energy[4] is ~16.5 kcal mol^{-1} and $\Delta H_5°$ is -9.5 kcal mol^{-1} provides an estimate of ~45 kcal mol^{-1} for the average Rh–C bond energy in 2. M–C bond energies are quite sensitive to steric effects,[5,6] and as a result the (OEP)Rh–CH_2 bond is undoubtedly stronger than the (OEP)Rh–$CH(CH_3)$ bond. As a working hypothesis we suggest that the Rh–CH_2– and Rh–$CH(CH_3)$– bond energies in 2 are approximately 50 and 40 kcal mol^{-1}, respectively.

$$\text{M–M} + CH_2{=}CH(R) \rightleftarrows \text{M—}CH_2CH(R)\text{—M} \quad (7)$$

$$\Delta H°_7 = (\text{M—M}) - 2(\text{M—C}) + 3({=}\text{C—H}) + ({=}\text{C—R}) + (\text{C}{=}\text{C}) - 3(\text{—C—H}_s) - (\text{—C—R}) - (\text{C—C}) \quad (8)$$

$$\Delta H°_7 \sim (\text{M—M}) - 2(\text{M—C}) + 63 \text{ kcal mol}^{-1} \quad (9)$$

$$\Delta G°_7 \text{ (298 K)} \sim (\text{M-M}) - 2(\text{M-C}) + 71 \text{ kcal mol}^{-1} \quad (10)$$

Scheme I. Mechanistic Schemes for a Nondissociative 1,2-Exchange Process

(a) Nonpolar Concerted (Symmetric Transition State)

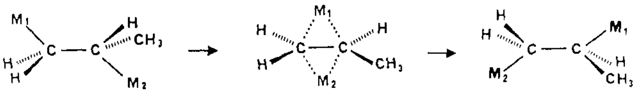

(b) Polar-two-step Process (Nonsymmetrical Transition State)

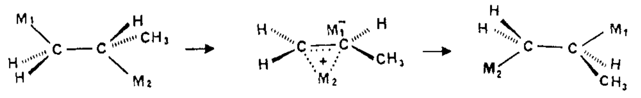

Kinetic–Mechanistic Study of the 1,2 Exchange of (OEP)Rh Groups in 2. The interchange of nonequivalent (OEP)Rh units ((1) and (2)) in (OEP)$Rh_{(1)}$–$CH_2CH(CH_3)$–$Rh_{(2)}$(OEP) (eq 11) is demonstrated by the broadening and subsequent merging of the porphyrin methine ^{1}H NMR resonances as the temperature is elevated (T = 270–320 K) (Figure 2) (eq 11).

$$(\text{OEP})\text{Rh}_{(1)}\text{-}CH_2CH(CH_3)\text{-Rh}_{(2)}(\text{OEP}) \rightleftarrows (\text{OEP})\text{Rh}_{(2)}\text{-}CH_2CH(CH_3)\text{-Rh}_{(1)}(\text{OEP}) \quad (11)$$

The chiral center in 2 provides a probe for the stereospecificity of the 1,2-interchange process. A nonstereospecific process would result in the diastereotopic hydrogens ($H_{(1)}$ and $H_{(2)}$) becoming equivalent. If the interchange of (OEP)Rh units or another process that occurs at a competitive rate results in the interchange of $H_{(1)}$ and $H_{(2)}$, then the dynamic process would first be manifested in the ^{1}H NMR by averaging the coupling constants ($J_{1,3}$ and $J_{2,3}$) and subsequently result in the merging of the $H_{(1)}$ and $H_{(2)}$ resonances as the temperature is elevated. A simulation of the ^{1}H NMR for the $H_{(2)}$ proton in 2 corresponding to this exchange case is illustrated in Figure 3 along with the observed spectra. Absence of a temperature dependence for the observed ^{1}H NMR patterns of $H_{(1)}$, $H_{(2)}$, and $H_{(3)}$ demonstrates that the 1,2 interchange of (OEP)Rh units is a stereospecific process. Either retention or inversion of configuration at both carbon centers would result in this observation, but only pathways that involve a double inversion can be readily envisioned.

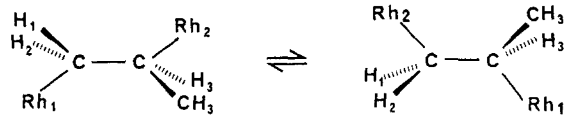

The stereospecific nature for reaction 11 indicates that the (OEP)Rh interchange is fast relative to dissociative processes that form localized organic radicals or carbonium ion centers such as (OEP)Rh—$CH_2\dot{C}H(CH_3)$ or (OEP)Rh—CH_2 $^+CH(CH_3)$. The observed activation enthalpy (ΔH^*_{11} = 12.4 kcal mol^{-1}) is too small to be associated with an unassisted Rh–C bond homolysis which for the specific example of compound 2 requires a minimum of approximately 40 kcal mol^{-1} but a neighboring group anchimeric effect of the (OEP)Rh unit could assist Rh–C bond homolysis or heterolysis and also produce stereospecificity for the 1,2 exchange. Although a dissociative process corresponding to the reverse of reaction 5 must occur in this system,[2] it is probably not involved in the pathway responsible for the observed 1,2-exchange process. The relatively large negative entropy of activation for reaction 11 (ΔS^*_{11} = -10.7 cal K^{-1} mol^{-1}) provides clear evidence that a nondissociative pathway is used in accomplishing the 1,2 interchange in benzene. Two pathways that are compatible with the activation parameters and stereospecific nature of reaction 11 are illustrated in Scheme I.

A dyotropic process has been defined by Reetz[7,8] as a

---

(3) The bond energy estimates for the hydrocarbon fragments are obtained by using Laidler parameters. (Pedley, J. B.; Naylor, R. D.; Kirby, S. P. *Thermochemical Data of Organic Compounds*, 2nd ed.; Chapman and Hall: London, 1986; Table 50, p 592): (C=C) = 133.0, (C—C) = 85.4, (=C—C) = 88.5, (—C—H_s) = 97.3, (=C—H) = 101.2.

(4) Wayland, B. B.; Coffin, V. L.; Farnos, M. D. *Inorg. Chem.* **1988**, *27*, 2745.

(5) Halpern, J. *Acc. Chem. Res.* **1982**, *15*, 238.

(6) Ziegler, T.; Tschinke, V.; Becke, A. *J. Am. Chem. Soc.* **1987**, *109*, 1351.

(7) (a) Reetz, M. T. *Angew. Chem.* **1972**, *84*, 161. (b) Reetz, M. T. *Tetrahedron* **1973**, *29*, 2189. (c) Reetz, M. T.; Kliment, M.; Plachky, M.; Greif, N. *Chem. Ber.* **1976**, *109*, 2716. (d) Reetz, M. T. *Chem. Ber.* **1977**, *110*, 954.

reaction that occurs by intramolecular positional interchange of σ-bonded groups. Several dyotropic processes that involve 1,2 interchanges similar to reaction 11 include reactions of 1,2-bis(silyl)ethane derivatives,[7] $5\alpha,6\beta$-dibromo steroids,[9] α,β-dibromocyclohexanes,[10] and dinuclear (μ-aldehyde)zirconocene complexes.[11,12] Concerted 1,2 exchange of hydrogen and substituents in ethanes has been the subject of several theoretical studies.[13–15] The extremely large activation barrier (150–200 kcal mol^{-1})[13] for this process in ethane primarily arises from the high energy associated with the symmetrical hydrogen-bridged (D_{2h}) transition state relative to the staggered D_{3d} structure for ethane. The highest occupied molecular orbital of the D_{2h} transition state is essentially a filled π^* orbital of ethene dianion ($C_2H_4^{2-}$), and this MO has been identified as the origin of the high energy associated with the symmetrically bridged (D_{2h}) structure (structure I). A migrating group that has available π-acceptor orbitals such as empty dπ orbitals (structure II) can stabilize the symmetrical transition state and reduce the barrier for a concerted 1,2 exchange.[13,14] Interaction of the filled π^* of $(C_2H_4)^{2-}$ with empty dπ orbitals probably explains the structure[16,13b] and dynamics[11] observed for organozirconium(IV) complexes and could be invoked for 1,2-bis(silyl) and α,β-dibromo derivatives, but this type of interaction is not available to rhodium(III) which has filled dπ (d_{xz^2}, d_{yz^2}) orbitals. Stabilization of a symmetrically bridged structure in the (OEP)Rh case (OEP)Rh–CH$_2$CH(CH$_3$)–Rh(OEP) (**2**) would have to involve the rhodium $5p_{x,y}$ which are used in σ bonding to the porphyrin or an interaction with the porphyrin π^* orbitals. It seems unlikely that these secondary π interactions could account for the remarkably low activation energy barrier for 1,2 (OEP)Rh exchange in **2** (eq 11) ($\Delta H^*_{11} = 12.4$ kcal mol^{-1}).

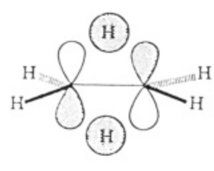

I

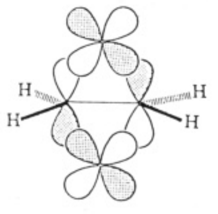

II

The currently available experimental evidence cannot distinguish between a concerted and two-step process (mechanism a or b), but we believe that a multistep mechanism with an unsymmetrical transition state is more probable. A short-lived tight ion pair intermediate has been proposed in the conversion of $5\alpha,6\beta$-dibromo steroids to the $5\beta,6\alpha$ isomers.[9] This type of reaction intermediate is attractive for the interchange of (OEP)Rh groups in **2** because [(OEP)Rh(III)]$^+$ is known to form a stable ethene π complex.[17] If this mechanistic feature is correct, then any substituent that can form an alkene π complex as a cation should provide a facile pathway for 1,2-migration reactions.

Experimental Section

Reagents. [Rh(CO)$_2$Cl]$_2$, octaethylporphine (OEPH$_2$), and propene were used as purchased from Aldrich. Benzene-d_6 from Aldrich was dried over Na/benzophenone, degassed by freeze–pump–thaw cycles, and stored over Na/benzophenone.

(OEP)Rh(H) and [(OEP)Rh]$_2$ were prepared by literature methods.[1,18]

Thermodynamic Study. Solid [(OEP)Rh]$_2$ (2–3 mg) was weighed and placed in an NMR tube adapted with a high vacuum stopcock. Dried and degassed benzene-d_6 was vacuum distilled into the NMR tube. The tube was subsequently pressurized with propene and sealed.

Variable-temperature ^{1}H NMR spectra were obtained on an IBM-Bruker AF200SY or IBM Bruker WP200SY spectrometer equipped with a Bruker VI-1000 temperature controller. The probe was cooled with a FTS systems refrigerator unit equipped with a temperature controller. The temperatures in the sample were measured with external sample of methanol (below ambient) and ethylene glycol (above ambient).

The samples were kept away from light prior to and during the experiment. NMR spectra were obtained at 0.5–2 h intervals until three consecutive spectra showed no further changes in the relative areas of the peaks. Concentrations of **1**, **2**, and propene were obtained by using the integrated intensity of the porphyrin methine and alkene hydrogens, respectively. Thermodynamic parameters were obtained from a least-squares fit of ln K vs T^{-1} (K = [**2**]/[**1**][propene]).

Kinetic Study. [(OEP)Rh]$_2$ (2–3 mg) was placed in an NMR tube adapted with a high vacuum stopcock, and dried, degassed benzene-d_6 was vacuum distilled into the tube. The NMR tube was then pressurized with excess propene and sealed.

The activation enthalpy and activation entropy were determined by measuring changes in the methine ^{1}H NMR line shape as a function of temperature. The porphyrin methine hydrogen full line shape for the interchanging (OEP)Rh groups in **2** was simulated as an equal population two-site exchange case without coupling by using the DNMR5 program.[19]

NMR Parameters for 2, 3, and 4. (OEP)Rh–CH$_2$CH(CH$_3$)–Rh(OEP) (**2**): ^{1}H NMR (C$_6$D$_6$, 294 K) δ 9.40 (s, CH, 4 H), 9.27 (s, CH, 4 H), 3.97 (q, CH_2CH$_3$, 16 H), 3.73 (q, CH_2CH$_3$, 16 H), 1.79 (t, CH$_2$CH_3, 24 H), 1.67 (t, CH$_2$CH_3, 24 H), −8.68 (d, CHCH_3, 3 H), −9.89 (m, CHCH$_3$, 1 H), −10.36 (m, CH_1H$_2$, 1 H), −11.25 (m, CH$_1$$H_2$, 1 H). (OEP)Rh—CH$_2$CH═CH$_2$ (**3**): ^{1}H NMR (C$_6$D$_6$): δ 10.22 (s, CH, 4 H), 3.71 (m, CH_2CH$_3$, 16 H), 1.90 (t, CH$_2$CH_3, 24 H), −4.50 (d of d, RhCH_2, 2 H), +0.08 (m, CH═, 1 H), 2.64 (br d of d, ═CH$_2$, 1 H). (OEP)Rh–CH$_2$CH$_2$CH$_3$ (**4**): ^{1}H NMR (C$_6$D$_6$): δ 10.23 (s, CH, 4 H), 3.94 (q, CH_2CH$_3$, 16 H), 1.92 (t, CH$_2$CH_3, 24 H), −5.60 (t of d, Rh–CH_2, 2 H), −4.58 (m, CH_2CH$_3$, 2 H), −2.14 (t, CH$_2$CH_3, 3 H).

Acknowledgment. We gratefully acknowledge support of this work by the National Science Foundation and the Department of Energy, Division of Chemical Sciences, Offices of Basic Energy Sciences, through Grant DE-FG02-86ER13615. We also thank Dr. George Furst for guiding the NMR simulations.

Registry No. **1**, 63439-10-1; **2**, 120418-74-8; **3**, 120418-75-9; **4**, 57584-04-0; CH$_2$═CHCH$_3$, 115-07-1.

---

(8) Reetz, M. T. *Adv. Organomet. Chem.* **1977**, *16*, 33.

(9) (a) Grob, C. A.; Winstein, S. *Helv. Chim. Acta* **1952**, *99*, 782. (b) Barton, D. H. R.; Head, A. J. *J. Chem. Soc.* **1956**, 932.

(10) Barili, P. L.; Bellucci, G.; Berti, F.; Marioni, A.; Marsili, A.; Morelli, I. *J. Chem. Soc., Chem. Commun.* **1970**, 1437.

(11) Gell, K. I.; Williams, G. M.; Schwartz, J. *J. Chem. Soc., Chem. Commun.* **1980**, 550.

(12) (a) Erker, G. *Acc. Chem. Res.* **1984**, *17*, 103. (b) Erker, G.; Kropp, K. *Chem. Ber.* **1982**, *115*, 2437.

(13) a) Hoffman, R.; Williams, J. E., Jr. *Helv. Chim. Acta* **1972**, *55*, 1, 67. (b) Tatsumi, K.; Hoffman, R. *J. Am. Chem. Soc.* **1981**, *103*, 3328.

(14) Reetz, M. T. *Tetrahedron* **1973**, *29*, 2189.

(15) Gimarc, B. M. *J. Am. Chem. Soc.* **1973**, *95*, 1417.

(16) Kaminsky, W.; Kopf, J.; Sinn, H.; Vallmer, H. J. *Angew. Chem.* **1976**, *88*, 688.

(17) Wayland, B. B.; Van Voorhees, S. L.; Del Rossi, K. J. *J. Am. Chem. Soc.* **1987**, *109*, 6513.

(18) (a) Setsune, J.; Yoshida, Z.; Ogoshi, H. *J. Chem. Soc., Perkin Trans. 1* **1982**, 983. (b) Ogoshi, H.; Setsune, J.; Omura, T.; Yoshida, Z. *J. Am. Chem. Soc.* **1975**, *97*, 6461.

(19) (a) Sandstrom, J. *Dynamic NMR Spectroscopy*; Academic Press: New York, 1982; p 12. (b) *QCPE* **1978**, No. 365.